Arch. Metall. Mater., Vol. 61 (2016), No 2B, p. 1083–1088

DOI: 10.1515/amm-2016-0182

M. PASTUSZAK*#, G. CIEŚLAK*, A. DOBKOWSKA*, J. MIZERA*, K.J. KURZYDŁOWSKI*

THE DEVELOPMENT OF RAPIDLY SOLIDIFIED MAGNESIUM – COPPER RIBBONS

The aim of the present work was to plan and carry out an experiment consisting of amorphization of industrial magnesium alloy WE 43 (Mg – 4 Y – 3 RE – 0.5 Zr) modified by the copper addition. Investigated alloy modified with 20% of copper was rapidly quenched with the use of melt spinning technique. The effects of cooling rate on the structure and properties of the obtained material were extensively analyzed. The structure and phase analysis of samples were examined using X-ray diffraction method (XRD) while the thermal stability of the samples was determined by differential scanning calorimetry (DSC). Microstructure observations were also conducted. The microhardness tests ($HV_{0.02}$) and corrosion resistance tests were carried out to investigate the properties of the material. Corrosion resistance measurements were held using a typical three-electrode system. As the result of the research, the effect of cooling rate on microstructure and properties of investigated alloy was determined.

Keywords: magnesium-based alloys, rapid solidification, microstructure, mechanical properties, corrosion properties

1. Introduction

Magnesium-based alloys are attractive in many industries, in branches such as motorization or aerospace engineering. The main advantages of those alloys are low density and high strength, however, they still show a poor corrosion resistance [1-3]. One of the modern branches where they are used is biomedicine, where magnesium alloys play an important role as parts of implants or in the manufacturing of the medical equipment. For this purpose, magnesium alloys are prepared in the form of ribbons with amorphous structure with the use of rapid solidification. Due to remarkable effects of this method on microstructure, application of this technique to magnesium-based alloys can enhance mechanical and physical properties when compared to the conventional magnesium-based alloys. Previous results have shown that rapid quenching of those materials can improve their strength, ductility, corrosion resistance and thermal stability [4-6].

Recent studies have demonstrated that the addition of certain metals to magnesium-based alloys is effective in increasing the glass forming ability. Positive effects of La, Ce, Pd, Pr, Y and Ca addition on the properties and microstructure of magnesium-based alloys have been reported [4,7-10]. S. Yamuara et. al. [10] reported that an amorphous single phase can be obtained by the addition of the small amounts of Ca, La or Pd to the Mg_2Ni alloy. They also noticed that the Pd addition is more effective than this of two other elements. Q. Zheng, et. al. [11] reported that the partial substitution of Y by Nd in the Mg-Cu-Y alloy improved the glass transition of the material. Improvement of mechanical and physical properties of amorphous materials were noticed in both cases.

No records concerning the influence of Cu on the microstructure and properties of magnesium-based ribbons have been found in the literature. Also, the aim of this paper is to investigate the influence of Cu addition on the microstructural changes, as well as on the mechanical and corrosive properties of rapidly solidified ribbons produced from WE 43 alloy.

2. Material

In this work the microstructures and certain properties of the ribbons made from WE43(Mg – 4 Y – 3 RE – 0.5 Zr) magnesium-based alloy are described. The influence of Cu addition on the microstructure and properties has also been investigated. For this purpose, two types of melt – spun ribbons were obtained: from WE43 magnesium alloy and WE43 magnesium alloy with the addition of technically pure Cu. WE43 and WE43 + Cu alloys were manufactured in an Ar atmosphere by arc melting in a vacuum furnace. Following, rapidly solidified (RS) ribbons were prepared by melt spinning technique. The width of received samples was about 4 mm and thickness about 30 μm. It has been proved, that, the cooling rate of the process is a critical factor, as it ensures the quality of the amorphous phase formation. Based on the literature data, authors had chosen different wheel speeds which controlled the cooling rate. Magnesium ribbons were produced with wheel speed 10, 12,5, 15 and 17,5 m/s and the ejection pressure of 200 mbar.

* WARSAW UNIVERSITY OF TECHNOLOGY, FACULTY OF MATERIALS SCIENCE AND ENGINEERING, 141 WOLOSKA STR., WARSAW, POLAND

Corresponding author: monika.pastuszak@wimpw.edu.pl

3. Methodology

Firstly, an amorphous nature and phase identification of analyzed materials were examined with the use of X-ray diffraction method (XRD). The measurements were carried out on the diffractometer (Bruker D8 Advance) with CuK_{α} radiation at 35 kV and 40 mA. After that, the thermal stability of randomly selected samples was examined by differential scanning calorimetry (DSC) with the use of DSC 8000 Perkin Elmer device at the heating rate of 40°K/min. In order to provide a pictorial evidence of microstructures of analyzed samples, scanning electron microscopy (SEM) observations were done. Observed samples were prepared with the standard metallographic procedure, including cutting, mounting, grinding and polishing. They were grounded with 1200 grit papers, mechanically polished with a diamond suspension and etched with the use of the 3% Nital etching reagent. Observations were done with the use of TM 1000 microscope at an accelerating voltage 15 kV.

Following the microstructure observations, selected properties of the ribbons were measured. To describe the mechanical properties the micro hardness tests on the profiles of samples were done and the Hanneman Microhardness Tester with 20 g of the load was used. All the reported values were the average of at least 5 individual measurements. To characterize the corrosion properties, the potentiodynamic tests were conducted in 3,5% NaCl solution at ambient temperature. The corrosion measurements were conducted in a typical three electrode system: a stationary specimen as a working electrode (WE), platinum as a counter electrode (CE) and a saturated calomel electrode as a reference electrode (RE). The tests were made at a scan rate of 10 mV/s, on the AutoLab PGSTAT 100 equipment.

4. Results

4.1. Structure Investigations

XRD patterns obtained for rapidly solidified WE43 and WE43 + Cu ribbons are given in Fig. 1-4 and Fig. 5-8, respectively. In the microstructures of all analyzed ribbons prepared from WE43 alloy diffraction peaks of Mg – solid solution occurred only. In the case of WE43 modified with Cu, diffraction lines of Mg – solid solution and $CuMg_2$ phase were present.

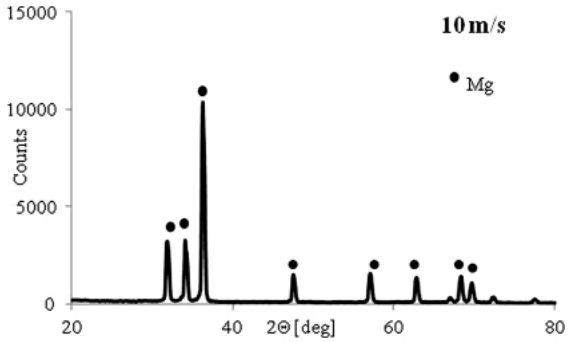

Fig. 1. XRD pattern obtained for WE 43 ribbon rapidly solidified with wheel speed 10 m/s

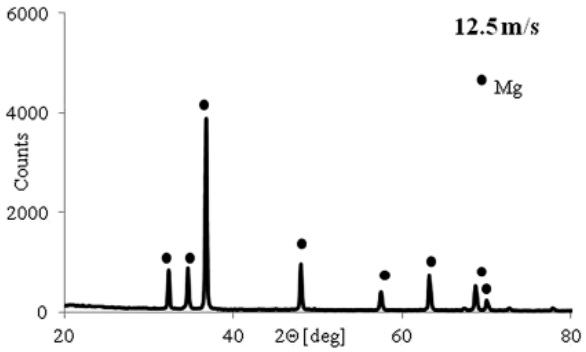

Fig. 2. XRD pattern obtained for WE 43 ribbon rapidly solidified with wheel speed 12,5 m/s

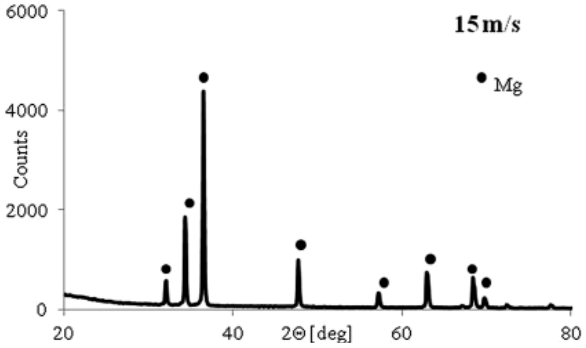

Fig. 3. XRD pattern obtained for WE 43 ribbon rapidly solidified with wheel speed 15 m/s

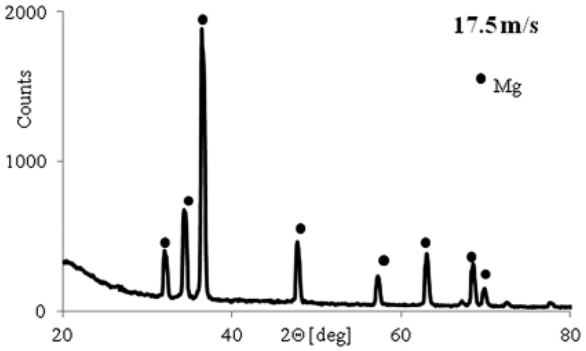

Fig. 4. XRD pattern obtained for WE 43 ribbon rapidly solidified with wheel speed 17,5 m/s

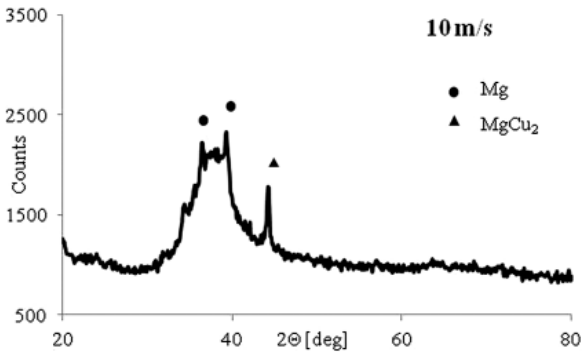

Fig. 5. XRD pattern obtained for WE 43 + Cu ribbons rapidly solidified with wheel speed 10 m/s

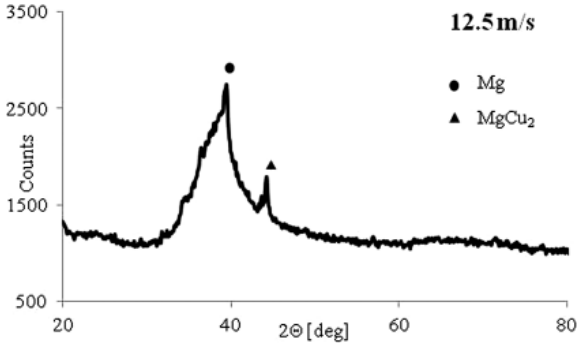

Fig. 6. XRD pattern obtained for WE 43 + Cu ribbons rapidly solidified with wheel speed 12,5 m/s

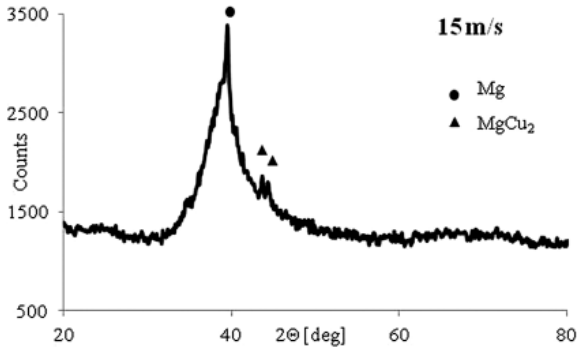

Fig. 7. XRD pattern obtained for WE 43 + Cu ribbons rapidly solidified with different wheel speed 15 m/s

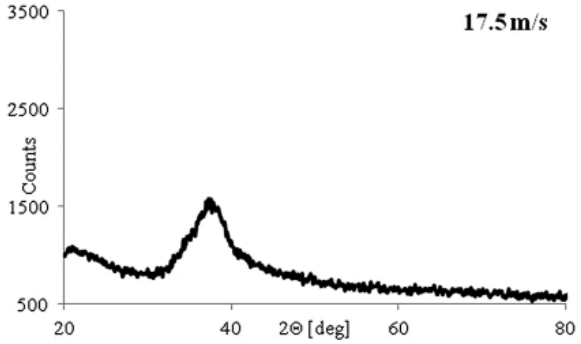

Fig. 8. XRD pattern obtained for WE 43 + Cu ribbons rapidly solidified with wheel speed 17,5 m/s

The peaks observed on the diagrams show that all analyzed ribbons obtained from base alloy are in a crystalline form (Fig. 1-4). A different situation occurs when microstructure of base alloy was modified with the addition of Cu. Apart from the ribbon cooled with the speed of 17,5 m/s (Fig. 8), the microstructures of samples enriched with Cu (Fig. 5-7) are described by a broad diffraction peak and crystalline peaks also. It indicates that these microstructures exhibit both amorphous and crystalline phases. The ribbon modified with a wheel speed of 17,5 m/s exhibits a diffuse diffraction maxima peak which is characteristic for an amorphous structure and there are none of the clearly visible diffraction peaks corresponding to crystalline phases. The aforementioned facts can confirm the existence of fully amorphous microstructure in this ribbon.

4.2. Differential scanning calorimetry

Due to fully crystalline microstructure observed in all WE43 ribbons, thermal stability was only examined for ribbons cooled with the speed of 15 m/s.

The results are given in Fig. 9a. The shape of presented diagram indicates the presence of endothermic effects associated with melting. DSC results for WE43 + Cu ribbon cooled with a wheel speed of 15 m/s are shown in Fig. 9b. On the DSC curve, we can observe three endothermic effects connected with different melting points of the obtained phases in the rapidly solidified ribbons and two exothermic peaks corresponding to crystallization of the amorphous phase.

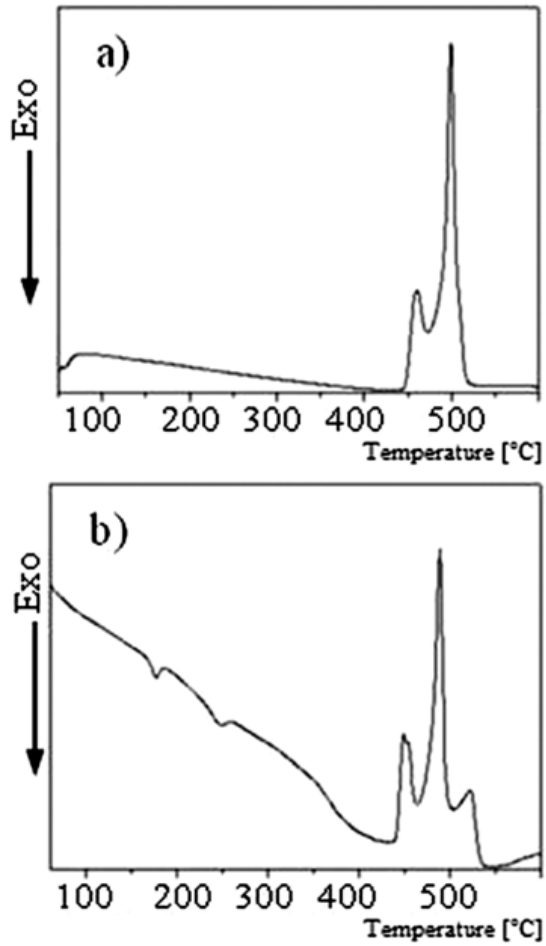

Fig. 9. DSC diagram obtained for ribbons rapidly solidified with wheel speed 15 m/s a) WE43 and b) WE 43 + Cu

4.3. Microstructure analysis

Microstructures of melt spun ribbons are presented in Figures 10 and 11. The microstructures of WE43 alloy ribbons melt spun at wheel speeds of 10 m/s, 12,5 m/s, 15 m/s and 17,5 m/s are given in Fig. 10a-d, respectively. As the figures 10a-d show, the microstructures of all above mentioned samples are characterized by equiaxed grain structures at the surface with higher cooling rate, followed by the elongated grains on the other side of ribbons.

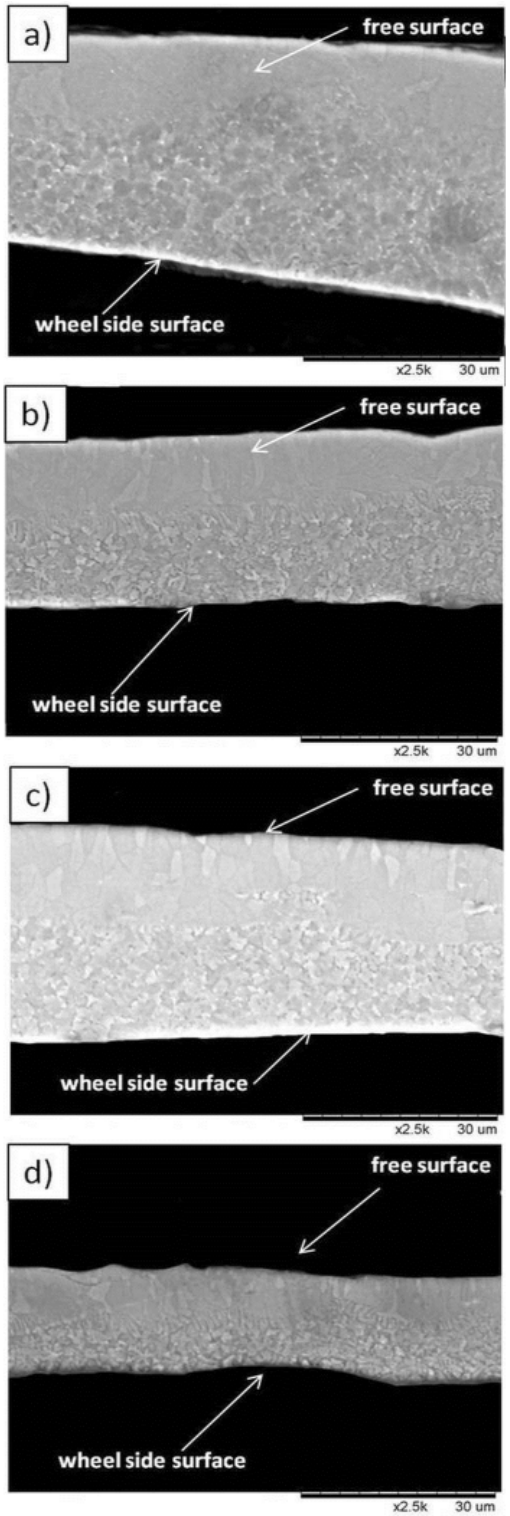

Fig. 10. SEM photos obtained for WE 43 ribbons with different wheel speeds a) 10 m/s, b) 12,5 m/s, c) 15 m/s, d) 17,5 m/s

It is well known that the addition of some elements to the base alloy can have a strong influence on its microstructure. In this instance, the addition of Cu caused the replacement of equiaxed grains observed in the microstructures of WE43 ribbons (Fig. 10) with a dendritic structure presented in Fig. 11. Moreover, composite dendritic microstructures in the amorphous matrix can be observed in Fig. 11a-c. This indicates that the microstructures of ribbons cooled with the rates of 10 m/s, 12,5 m/s and 15 m/s consist of amorphous and crystalline phases. The microstructure of the ribbon cooled with the wheel speed of 17,5 m/s is almost featureless – it is possible that the fully amorphous state has been formed (Fig. 11d). There is a noticeable contrast which may origin from specimen preparation but may also come from partial crystallization. The microstructural observations of the ribbons confirmed the results obtained from XRD and DSC methods.

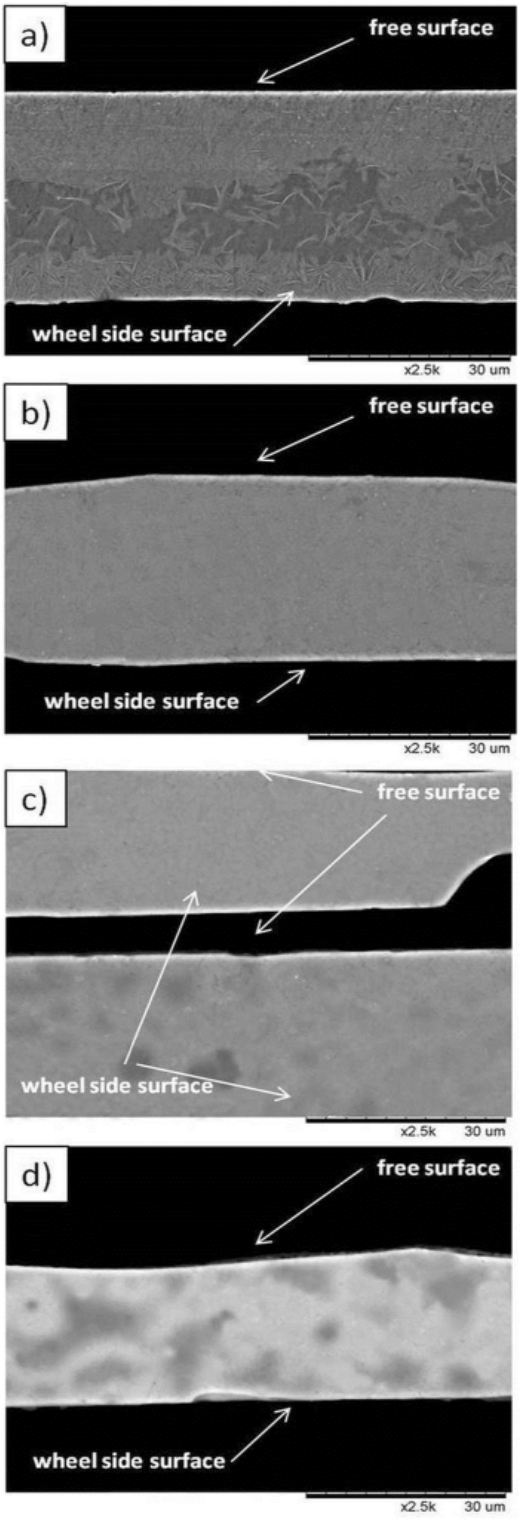

Fig. 11. SEM photos obtained for WE 43 + Cu ribbons with wheel speeds a) 10 m/s, b) 12,5 m/s, c) 15 m/s, d) 17,5 m/s

4.4. Mechanical properties

As the diagram shows, a slight hardening with the increase of cooling rate for both types of ribbons was observed (Fig. 12). The values of the micro hardness of WE43 ribbons were about 87, 95, 103 and 104 $HV_{0.02}$ for the samples obtained with wheel speeds of 10, 12,5, 15 and 17,5 m/s, respectively. It should be noted, that the addition of Cu to the WE43 alloy improves the mechanical properties of ribbons. The micro hardness of WE43 + Cu ribbons was 146, 164, 198 and 337 $HV_{0.02}$ for the wheel speeds of 10, 12,5, 15 and 17,5 m/s, respectively.

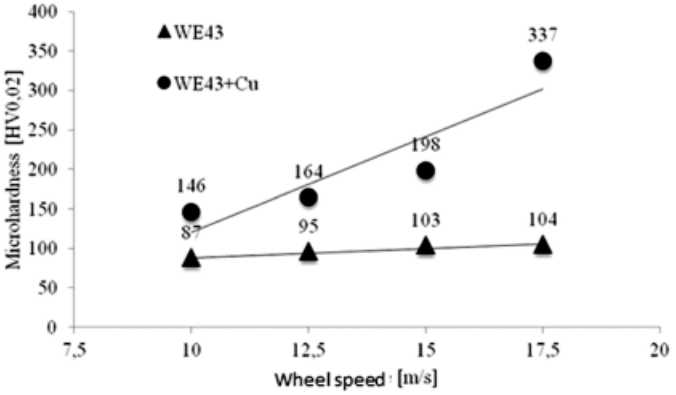

Fig. 12. Relationship between the microhardness and the wheel speed of WE 43 and WE 43 + Cu ribbons

4.5. Corrosion resistance

Potentiodynamic polarization curves obtained for analyzed materials are given in Fig. 13. As the diagram shows, the shape of potentiodynamic curves is similar for all the ribbons and they do not demonstrate any ability to passivate in 3,5% NaCl solution. It should be noted, that the addition of Cu to WE43 alloy caused the displacement of corrosive potentials (E_{corr}) towards positive values.

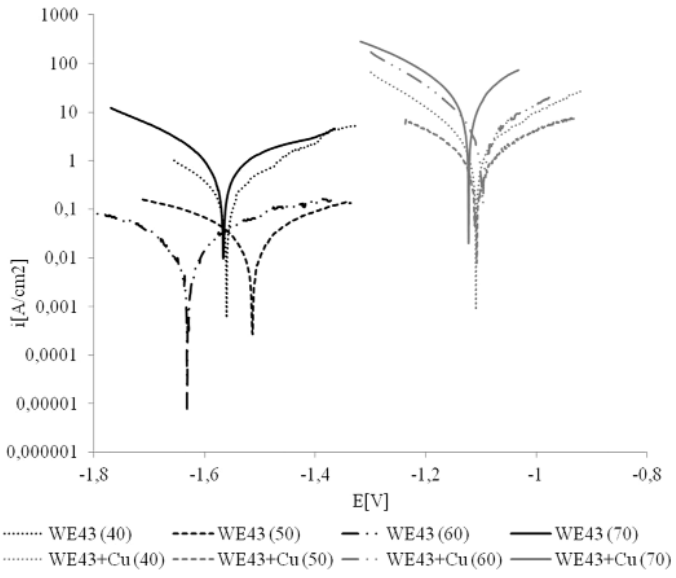

Fig. 13. Potentiodynamic polarization curves obtained for WE 43 and WE 43 + Cu ribbons

As the Table 1 shows, E_{corr} established values from – 1,57, – 1,51, – 1,62 to – 1,55 V for ribbons obtained from WE43 with cooling rates of 10, 12,5, 15 and 17,5 m/s, respectively. E_{corr} for ribbons produced from WE43 + Cu alloy oscillated around – 1,1 V for all the examined samples. It can be noticed that values of current density for ribbons produced from WE43 are lower than in the case of WE43 + Cu. Based on these results it could be assumed that the Cu addition enhanced corrosion resistance of the analyzed ribbons. However, the values of current density suggest that strong microgalvanic processes may have occurred in the microstructures with Cu addition.

TABLE 1

Standard corrosive parameters obtained from potentiodynamic technique

	WE 43				**WE 43 + Cu**			
	10 m/s	**12.5 m/s**	**15 m/s**	**17.5 m/s**	**10 m/s**	**12.5 m/s**	**15 m/s**	**17.5 m/s**
E_{corr} [V]	–1,57	–1,51	–1,62	–1,55	–1,1	–1,1	–1,09	–1,1
i_{corr} [A/m^2]	0,2	0,04	0,03	0,9	2,1	1,2	4,1	18

5. Conclusions and summary

The aim of this work was to evaluate the microstructures of rapidly solidified ribbons produced from two kinds of magnesium alloys: WE43 and WE43 with Cu addition. As the X-ray diffraction measurements confirmed, Mg – solid solution appeared in the microstructures of WE43 ribbons, while Mg – solid solution and $CuMg_2$ phase were present in WE43 + Cu ribbons. The fully crystalline structure was observed in WE43 ribbons while the Cu addition caused the appearance of an amorphous phase. DSC results and SEM observations confirmed that the Cu addition had an influence on increasing the glass formability of the analyzed materials. It should be noted that the Cu addition improved the mechanical properties and corrosion resistance of the alloy. Moreover, besides the chemical composition, another parameter was also taken into consideration during the research, namely cooling rate, which turned out to have a significant influence on the microstructural evolution, mechanical and corrosive properties. The higher the cooling rate, the more significant the enhancement of the above mentioned properties.

REFERENCES

[1] P. Drzymała, Microstructural conditions of plastic deformation of Mg-based metal alloys. Ph.D. thesis, Institute of Metallurgy and Materials Science, Polish Academy of Science, June (2015).

[2] W. Jin, J. Fan, H. Zhang, Y. Liu, H. Dong, and B. Xu, J. Alloys Compd. **646**, 1-9 (2015).

[3] K. Kubok, Characterization of microstructure and properties of biodegradable alloys from the Mg-Zn-Ca. Ph.D. thesis, Institute of Metallurgy and Materials Science, Polish Academy of Science, June (2015).
[4] Y. Li, H.Y. Liu, J. Mater. Process. Technol. **48**, 483-487 (1995).
[5] X.L. Zhang, G. Chen, T. Bauer, Intermetallics **29**, 56-60 (2012).
[6] S.H. Makoto Sugamata, Junichi Kaneko, Mater. Sci. Eng. A **226-228**, 861-866 (1997).
[7] S. Yamaura, H. Kim, H. Kimura, A. Inoue, Y. Arata, J. Alloys Compd. **347**, 239-243 (2002).
[8] S.I. Yamaura, H. Kimura, A. Inoue, J. Alloys Compd. **358**, 173-176 (2003).
[9] Y. Guangyin, L. Manping, D. Wenjiang, A. Inoue, Mater. Sci. Eng. A **357**, 314-320 (2003).
[10] S.I. Yamaura, H.Y. Kim, H. Kimura, A. Inoue, Y. Arata, J. Alloys Compd. **339**, 230-235 (2002).
[11] Q. Zheng, H. Ma, E. Ma, J. Xu, Scr. Mater. **55**, 541-544 (2006).